

Oxygen-rich disk in the V778 Cyg system resolved

R. Szczerba¹, M. Szymczak², N. Babkovskaia³, J. Poutanen³, A.M.S. Richards⁴, and M.A.T. Groenewegen⁵

¹ N. Copernicus Astronomical Center, Rabańska 8, 87-100 Toruń, Poland

² Toruń Centre for Astronomy, Nicolaus Copernicus University, Gagarina 11, 87-100 Toruń, Poland

³ Astronomy Division, P.O.Box 3000, University of Oulu, FIN-90014 Oulu, Finland

⁴ Jodrell Bank Observatory, University of Manchester, Macclesfield, Cheshire SK11 9DL, UK

⁵ Instituut voor Sterrenkunde, PACS-ICC, Celestijnenlaan 200B, B-3001 Leuven, Belgium

Received / Accepted

Abstract. The 22 GHz water maser emission from the silicate carbon star V778 Cyg has been mapped using MERLIN with an astrometric accuracy of 25 mas. The maser complex is displaced by \sim 190 mas from the position of the C-star measured 10 years previously. Our simulations show that this position difference is unlikely to be due to proper motion if V778 Cyg is at the assumed distance of 1.4 kpc. The maser components form a distorted S-shaped structure extended over \sim 18 mas along a position angle of -20° with a clear velocity gradient. We argue that the observed water maser structure can be interpreted as an O-rich disk around the secondary in the V778 Cyg binary system.

Key words. stars: AGB and post-AGB – stars: carbon – stars: chemically peculiar – masers

1. Introduction

The silicate emission features at about 10 and $18\mu\text{m}$ are characteristic of O-rich dust envelopes. Surprisingly, these features were also discovered in the IRAS LRS data for some optically classified carbon stars (Little-Marenin 1986; Willems & de Jong 1986), later termed silicate carbon stars. The detection of silicate emission from these stars suggests that their relatively close surroundings contain O-based dust, in spite of their photospheric chemical composition which shows $\text{C}/\text{O} > 1$. An additional argument for the persistence of O-rich material comes from the detection of water and OH maser lines towards some silicate carbon stars (e.g. Little-Marenin et al. 1994; Engels 1994; Little-Marenin et al. 1988).

Little-Marenin (1986) has proposed that silicate carbon stars are binaries consisting of a C-rich and O-rich giants. However, extensive observations (e.g. Lambert et al. 1990; Engels & Leinert 1994) did not show any evidence for an O-rich giant in these sources. Willems & de Jong (1986) proposed that silicate carbon stars were formed very recently due to a thermal pulse which changed the chemistry of the star from O- to C-rich and that the O-rich material ejected before and during the thermal pulse gives the observed silicate features. However, the Infrared Space Observatory (ISO) spectra showed that during the 14-year time interval between IRAS and ISO missions the shape and intensity of the silicate features in V778 Cyg did not change at all (Yamamura et al. 2000). The stability of the infrared features suggests that O-rich material is located in some stable configuration and that the model of a fast transition from

O- to C-rich star cannot apply, as the silicate features should diminish in strength quite rapidly. Presently, the most widely accepted scenario which is able to explain this phenomenon is a binary system composed of a C-star and an unseen, most likely main-sequence, companion with a reservoir of O-rich material (Morris et al. 1987; Lloyd Evans 1990). Yamamura et al. (2000) argued that the dust responsible for the observed silicate features is stored in a disk around the companion.

To test the above mentioned hypotheses we carried out, successfully, high angular resolution observations of water masers towards V778 Cyg. Previous observations revealed only that the unresolved radio emission coincides within $0\farcs5$ with the position of the optical star (Deguchi et al. 1988, Colomer et al. 2000). We also present a simple quantitative interpretation of the observed structure based on a Keplerian disk model.

2. Observations and data reduction

The observations were taken on 2001 October 12/13 under good weather conditions, using five telescopes of MERLIN. The instrument is described in detail by Diamond et al. (2003). The longest MERLIN baseline of 217 km gave a fringe spacing of 12 mas at 22 GHz. A bandwidth of 2 MHz was used divided into 256 spectral channels per baseline providing a channel separation of 0.105 km s^{-1} . The continuum calibrator sources were observed in 16 MHz bandwidth. The data were obtained in left and right circular polarisation. The velocities (V_{LSR}) were measured with respect to the local standard of rest.

We used the phase referencing method; 4 min scans on V778 Cyg were interleaved with 2 min scans on the source

2021+614 (at 3.8° from the target) over 11.5 h. The flux density of 2021+614 of 1.48 Jy was derived from observation of 4C39.25. At the epoch of observation the flux density of 4C39.25 was 7.5 ± 0.3 Jy (Terasranta 2002, private communication). This source was also used for bandpass calibration.

After initial calibration with the MERLIN software, the data were processed using the AIPS package (Greisen 1994). To derive phase and amplitude corrections for atmospheric and instrumental effects the phase reference source was mapped and self-calibrated. These corrections were applied to the V778 Cyg visibility data. The absolute position of the brightest feature at -15.1 km s^{-1} was determined. The clean components of this image were used as a model for phase self-calibration of this channel and the solutions were then applied to all channels. Each channel was then mapped and cleaned using a 12 mas circular restoring beam. We present results for total intensity (Stokes I) images. The map noise of $\sim 27 \text{ mJy beam}^{-1}$ in a line-free channel was close to the predicted thermal noise level.

To determine the position and the brightness of the maser components two dimensional Gaussian components were fitted to the emission in channel maps. The position uncertainty of this fitting depends on the signal to noise ratio in the channel map (Condon et al. 1989) and is lower than 1 mas for about 80% of the maser components towards V778 Cyg. The absolute position of the phase reference source is known within ~ 3 mas. The uncertainties in the absolute positions of the maser components are dominated by tropospheric effects and errors in the telescope positions. The former uncertainty was estimated by observing the phase rate on the point source 4C39.25 which appeared to introduce a position error of ~ 9 mas. Uncertainties in telescope positions of 1–2 cm cause a maser position error of ~ 10 mas. In order to check the position accuracy of the maser components we applied a reverse phase referencing scheme. Emission from 15 channels around the reference feature at -15.1 km s^{-1} was averaged and mapped. The map obtained was used as a model to self-calibrate the raw target data and these target solutions were then applied to the raw data of 2021+614. The position of the reference source was shifted by ~ 2 mas with respect to the catalog position. This indicates excellent phase connection when transferring solutions between 2021+614 and the masers of V778 Cyg. These factors imply that the absolute position accuracy of the maser source is $\lesssim 25$ mas.

3. Results and discussion

Single and unresolved maser emission components, brighter than $150 \text{ mJy beam}^{-1}$ ($\sim 5\sigma$), were found in 51 spectral channels. The overall distribution of the H_2O maser components in V778 Cyg is shown in Fig. 1. The absolute position of the reference feature at -15.1 km s^{-1} is given in Table 1 together with the optical position from the Tycho2 catalog (Hog et al. 2000). The maser components form a distorted S-like shape structure along the position angle of -20° . There is a clear velocity gradient along this structure with weak southern components blue-shifted in respect to the brightest northern components. The total angular extent of the maser emission is about 18 mas.

The inset in Fig. 1 shows the cross-correlation water maser spectrum towards V778 Cyg. The emission was dominated by

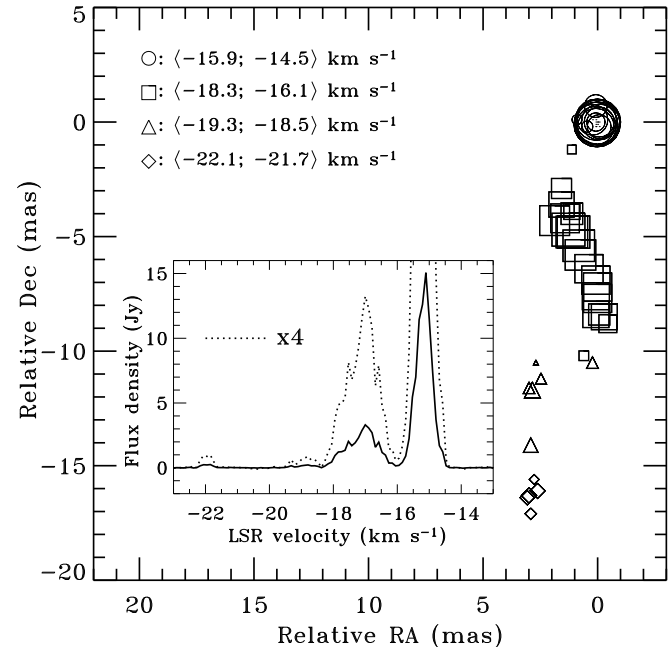


Fig. 1. Positions of the water maser components in V778 Cyg relative to the reference component at -15.1 km s^{-1} . The symbols correspond to the velocity ranges given in the upper left corner. The size of each symbol is proportional to the logarithm of peak brightness of the corresponding component. *Inset:* MERLIN spectrum of the H_2O maser emission in V778 Cyg. The dotted line shows the spectrum magnified by a factor of four to enlarge the weak features.

Table 1. Radio and optical coordinates (with errors) for V778 Cyg.

	Year	RA(J2000)	Dec(J2000)
MERLIN	2001	$20^{\text{h}}36^{\text{m}}07\text{s}3833 (\pm 0.0017)$	$60^{\circ}05'26''024 (\pm 0''.025)$
Tycho2	1991	$20^{\text{h}}36^{\text{m}}07\text{s}4022 (\pm 0.0029)$	$60^{\circ}05'26''154 (\pm 0''.040)$

a -15 km s^{-1} feature. Weak emission of about 200–250 mJy was seen at -22 and -19 km s^{-1} . The shape of the spectrum is roughly similar to that of the single dish spectra observed by Engels & Leinert (1994) and by Nakada et al. (1987).

3.1. Proper motion and the binary system

The angular separation between the positions of the C-star and the maser reference component (given in Table 1) is 192 mas (142 and 130 mas in RA and Dec, respectively). The observed difference seems to be significant ($\sim 3\sigma$ above the accuracy level in Table 1), but the epochs of optical and radio observations differ by about 10 years. The C-star would need a proper motion of $(\mu_\alpha \cos(\text{Dec}), \mu_\delta)$ close to $(-10, -10)$ mas yr^{-1} to produce the observed difference in radio and optical positions. The proper motion of V778 Cyg is not given in the Tycho2 catalog but Khrutskaya et al. (2004) estimate the proper motion of V778 Cyg to be in the range $\sim [(-8 \pm 2), (-4 \pm 8)]$ mas yr^{-1} .

This was further investigated using using the kinematic model of Groenewegen (2005, in preparation), which includes

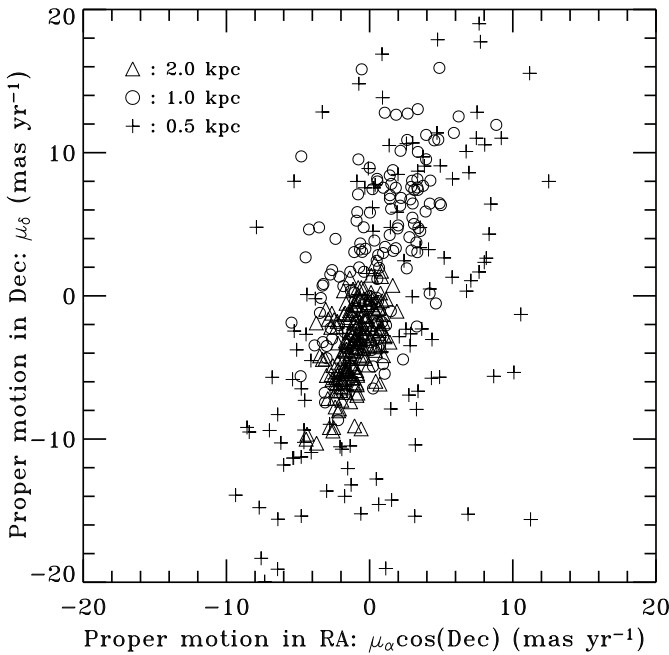


Fig. 2. The simulated proper motion for V778 Cyg for the assumed distance of 0.5, 1.0 and 2.0 kpc.

Galactic rotation, and, for the present calculations, random motions were drawn from Gaussian velocity ellipsoids with zero mean and dispersions, typical for giants, of 31, 21 and 16 km s⁻¹ (Delhaye 1965) in the *U*, *V*, *W* directions, respectively.¹

1000 simulations were performed to calculate proper motions and radial velocities in the direction of V778 Cyg ($l=95^\circ 6$, $b=+11^\circ 51$) for distances of 0.5, 1 and 2 kpc. Fig. 2 shows the results producing a V_{LSR} close to that of V778 Cyg, -20 ± 5 km s⁻¹, (determined from the heliocentric radial velocity of about -35 km s⁻¹, reported by Barbier-Brossat & Figon 2000). The most probable distance to V778 Cyg is $D \simeq 1.4$ kpc (Barnbaum et al. 1991; Yamamura et al. 2000), which does not produce the proper motions required to match the C-star with the radio position. Therefore, we believe that existing observations and simulations support a binary system model (Yamamura et al. 2000) and the water maser is associated with a companion star. However, observational errors are not negligible and simultaneous optical and radio observations are needed to confirm this hypothesis.

The water maser components at -15 , -17 , -19 and -22 km s⁻¹ have been detected several times during the last 15 years (Nakada et al. 1987, Engels & Leinert 1994, this paper). Comparisons of these observations show that changes in their radial velocities, ΔV , do not exceed 0.5 km s⁻¹. If the velocity

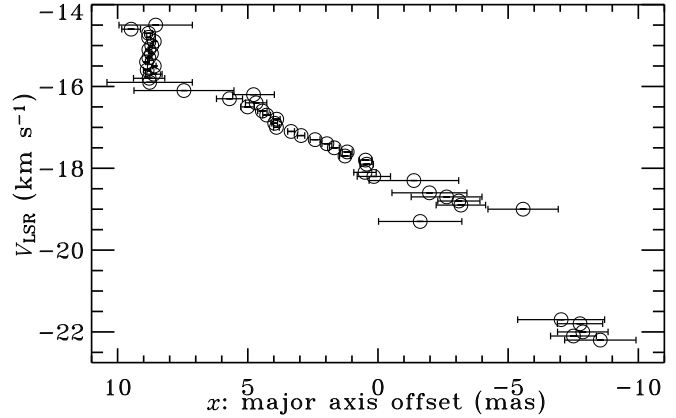


Fig. 3. The LSR velocity against the distance along the major axis for water maser components in V778 Cyg.

change is due to the orbital motion of the secondary (with its maser) around the carbon star (mass M_c), the rate of change is:

$$\frac{\Delta V}{\Delta t} \simeq \frac{GM_c}{d^2} \sin i, \quad (1)$$

where Δt is the time between observations, G is the gravitational constant and i is the inclination angle. Hence, for $i \simeq 90^\circ$, the distance d between the binary companions is given by:

$$d \gtrsim 75 \left(\frac{\Delta V}{0.5 \text{ km s}^{-1}} \right)^{-1/2} \left(\frac{\Delta t}{15 \text{ years}} \right)^{1/2} \left(\frac{M_c}{M_\odot} \right)^{1/2} \text{ AU}. \quad (2)$$

3.2. Water maser model

Fig. 3 shows the V_{LSR} of the water maser components versus major axis offset x , (V – x diagram). The major axis is defined by the two components with minimum and maximum velocities (Fig. 1) and the zero of angular offset marks the major axis center. Fig. 3 shows an almost linear velocity gradient with a greater velocity range per unit distance at the extremes. This is strongly characteristic of emission from an almost edge-on disc in Keplerian rotation (Shepherd & Kurtz 1999, Pestalozzi et al. 2004). We only detect one unresolved maser component per channel and therefore the apparent position of the component is along the line of sight of the greatest amplification at the V_{LSR} sampled by that channel. As unsaturated maser amplification is exponential, a relatively small change in optical depth arising from a differential velocity gradient produces strong domination by emission at the favoured velocity (derived rigorously in Pestalozzi et al. 2004 and references therein). In contrast, water masers associated with evolved-star jets (e.g. Miranda et al. 2001, Imai et al. 2002) typically show more fan-like structures with a less ordered velocity gradient which tends to be steepest in the centre, not at the limbs.

Assuming that the disk is Keplerian (radius $R \simeq 9$ mas $\simeq 12.6$ AU at distance to the object of 1.4 kpc), the line of sight velocity at impact parameter x relative to the V_{LSR} of the disk center is given by $V_x = V_K(x/R) \text{ km s}^{-1}$, where $V_K \simeq 3.5 \text{ km s}^{-1}$ is the Keplerian velocity at the observed disk edge. The lower limit, as the disk radius can be larger than the observed size of the water maser components distribution, to the central mass inside the disk is $M_s \simeq 0.17 (D/1.4 \text{ kpc}) M_\odot$.

¹ The following parameters also enter the model: a distance Sun-Galactic Center of 8.5 kpc (Kerr & Lynden-Bell 1986), Oort's constants of $A = 14.4 \text{ km s}^{-1} \text{ kpc}^{-1}$, $B = -12.0 \text{ km s}^{-1} \text{ kpc}^{-1}$, and higher order terms $\frac{d^2 \theta}{dr^2|_{R_0}} = -3.4 \text{ km s}^{-1} \text{ kpc}^{-2}$, $\frac{d^3 \theta}{dr^3|_{R_0}} = 2.0 \text{ km s}^{-1} \text{ kpc}^{-3}$ (Pont et al. 1994), and a Solar motion of 19.5 km s^{-1} in the direction $l=56^\circ 0$, $b=23^\circ 0$ (Feast & Whitelock 1997).

Yamamura et al. (2000) investigated the dust radiation from V778 Cyg in the infrared region. To obtain a good fit to the data, they needed silicate dust with temperature, T_d , around 300 K. They concluded that the total mass of silicates is $\sim 5 \times 10^{-7} M_\odot$. If the gas temperature, T_g , is determined by collisions with the dust (Goldreich & Kwan 1974), then it is of the same order of magnitude as T_d , provided that the radiative gas cooling does not exceed the gas heating. We assume here: $T_g = T_d = 300$ K.

The reference water maser component at -15.1 km s $^{-1}$ has a peak brightness of 24.4 Jy beam $^{-1}$, which corresponds to a lower limit on the brightness temperature of $T_R \simeq 6 \times 10^8$ K. If the maser emission is unsaturated, the optical depth in the maser line is $\tau = \ln[T_R/T_{ex}] \simeq 15.6$, where $T_{ex} \simeq 100$ K is the excitation temperature.

To find the disk half-thickness, H , we can use the equation of hydrostatic equilibrium (Shakura & Sunyaev 1973) $H/R = V_{t,H_2}/V_K$, where $V_{t,H_2} \simeq 1.3(T_g/300\text{ K})^{1/2}$ km s $^{-1}$ is the molecular hydrogen thermal velocity. For $V_K = 3.5$ km s $^{-1}$ and $R = 12.6$ AU, we estimate that $H \approx 5(T_g/300\text{ K})^{1/2}$ AU.

To make a more quantitative model of water maser emission from V778 Cyg we have used the method described in Babkovskaia & Poutanen (2004) assuming that the maser amplification length $S \approx 1.15 R \approx 14$ AU. We considered a slab consisting of a mixture of molecular hydrogen, water vapor and dust in a form of 1 μm astronomical silicate grains. To obtain the observed maser luminosity and the estimated above optical depth in a stable disk, we needed the hydrogen concentration $n_{H_2} = 10^8 \text{ cm}^{-3}$, the water-to-hydrogen mass ratio of $\approx 6 \times 10^{-3}$ and the dust-to-gas mass ratio of 0.05. Note, that increasing the radius of the disk we can get the observed maser luminosity for a smaller amount of water. From the above model the disk mass is $M_{\text{disk}} \simeq 2\pi R^2 H m_{H_2} n_{H_2} \simeq 4 \times 10^{-6} (T_g/300\text{ K})^{1/2} M_\odot$ (where m_{H_2} is the mass of the hydrogen molecule) and the total dust mass is about $2 \times 10^{-7} M_\odot$, which is close to a value reported by Yamamura et al. (2000). A more detailed model of O-rich disk in the V778 Cyg system, together with discussion of the free space parameters, will be presented in forthcoming full paper (Babkovskaia et al. 2005, in preparation).

4. Conclusions

We mapped the water maser emission from silicate carbon star V778 Cyg using MERLIN, revealing an S-shape structure of maser components at a position angle of -20° . The radio position obtained from MERLIN in 2001 is at an angular separation of 190 mas from the optical position of V778 Cyg given in the 1991 Tycho2 catalog. We argue that this cannot be explained by proper motion if V778 Cyg is at a distance of ~ 1.4 kpc and instead probably provides observational support for the binary system model of Yamamura et al. (2000). Simultaneous radio and optical measurements are needed to verify this model. The velocity changes of the main maser components over 15 years imply that the distance between the C-star and disk is at least 75 AU. The orbital period of V778 Cyg binary system is about 600 years. The water maser components have an almost linear distribution (similar to a very elongated distorted S) as projected on the sky and in the variation of V_{LSR} along the direction of elongation. We interpret this as an almost edge-on Keplerian

disk located around a companion star. We estimate that the central mass inside the disk is at least $0.17 M_\odot$ (for a distance of 1.4 kpc); if the disk material extends beyond the maser region the mass could be larger.

We considered a disk composed of silicates of temperature 300 K and assumed that gas has the same temperature. We estimated the disk scale-height to be $H \approx 5(T_g/300\text{ K})^{1/2}$ AU. Using more detailed modelling, we were able to get a stable disk and to reproduce the observed water maser luminosity and the estimated disk optical depth. Our model required a water-to-hydrogen mass ratio of $\approx 6 \times 10^{-3}$, a dust-to-gas mass ratio of 0.05 and molecular hydrogen concentration 10^8 cm^{-3} . The estimated total disk mass is $\sim 4 \times 10^{-6} M_\odot$ and the total dust mass $\sim 2 \times 10^{-7} M_\odot$. More detailed calculations will be reported in a future publication.

Acknowledgements. This work has been partly supported by grant 2.P03D.017.25 of the Polish State Committee for Scientific Research (RS), the Magnus Ehrnrooth Foundation, and the Finnish Graduate School for Astronomy and Space Physics (NB), and the Academy of Finland (JP). We are indebted to Dr. Francisco Colomer for the valuable comments improving the original manuscript.

References

- Babkovskaia, N., & Poutanen, J., 2004, A&A, 418, 117
- Barbier-Brossat, M., & Figon, P. 2000, A&AS, 142, 217
- Barnbaum, C., Morris, M., Likkel, L., & Kastner, J.H., 1991, A&A, 251, 79
- Colomer, F., Reid, M.J., Menten, K.M., & Bujarrabal, V. 2000, A&A, 355, 979
- Condon, J.J., Cotton, W.D., Greisen, E.W., et al., 1998, AJ, 115, 1693
- Deguchi, S., Kawabe, R., Ukita N., et al., 1988, ApJ, 325, 795
- Delhaye J., 1965, in Galactic structure, Stars and Stellar systems, Vol. 5, ed. A. Blaauw, M. Schmidt, University of Chicago Press
- Diamond, P.J., Garrington, S.T., Gunn, A.G., et al., 2003, MERLIN User Guide, ver. 3
- Engels, D., 1994, A&A, 285, 497
- Engels, D., & Leinert, Ch., 1994, A&A, 282, 858
- Feast M., & Whitelock P., 1997, MNRAS, 291, 683
- Goldreich, P., & Kwan, J., 1974, ApJ, 191, 93
- Greisen, E.W. (ed.), 1994, AIPS Cookbook, NRAO
- Hog, E., Fabricius, C., Makarov, V.V., et al., 2000, A&A, 355, L27
- Imai, H., Obara, K., Diamond, P.J., Omodaka, T., Sasao, T., 2002, Nature, 417, 829
- Kerr, F.J., & Lynden-Bell D., 1986, MNRAS, 221, 1023
- Khrutskaya, E.V., Khrutskaya, E.V., Khrutskaya, M.Y., & Bronnikova, N.M., 2004, A&A, 418, 357
- Lambert, D.L., Hinkle K.H., & Smith V.V., 1990, AJ, 99, 1612
- Little-Marenin, I.R., 1986, A&A, 307, L15
- Little-Marenin, I.R., Benson, P.J., & Dickinson, D.F., 1988, ApJ, 330, 828
- Little-Marenin, I.R., Sahai, R., Wannier, P.G., et al., 1994, A&A, 281, 451
- Lloyd Evans, T., 1990, MNRAS, 243, 336
- Miranda, L.F., Gómez, Y., Anglada, G., & Torrelles, J.M., 2001, Nature, 414, 284
- Morris, M., Guilloteau, S., Lucas, R., & Omont, A., 1987, ApJ, 321, 888
- Nakada, Y., Izumiura, H., Onaka, T., et al., 1987, ApJ, 323, L77
- Pestalozzi, M.R., Elitzur, M., Conway, J.E., & Booth, R.S., 2004, ApJ, 603, L113

Pont, F., Mayor, M., & Burki, G., 1994, A&A, 285, 415
Shakura, N.I., & Sunyaev, R.A., 1973, A&A, 24, 337
Shepherd, D.S., & Kurtz, S.E., 1999, ApJ, 523, 690
Willems, F.J., & de Jong T., 1986, ApJ, 309, L39
Yamamura, I., Dominik, C., de Jong, T., et al., 2000, A&A, 363, 629